Wear 271 (2011) 875–880

Mechanical and tribological properties of a sintered glass-ceramic compared to granite and porcelainized stoneware

S. Buchner[a], A. Mikowski[b], C.M. Lepienski[c], E.B. Ferreira[d], E.D. Zanotto[e], R.D. Torres[f], P. Soares[f,*]

[a] Physics Institute, Universidade Federal do Rio Grande do Sul, 91501-970 Porto Alegre, RS, Brazil
[b] Mobility Engineering Center, Universidade Federal de Santa Catarina, 89219-905 Joinville, SC, Brazil
[c] Physics Department, Universidade Federal do Paraná, 81531-990 Curitiba, PR, Brazil
[d] Department of Materials Engineering, Universidade de São Paulo, 13566-590 São Carlos, SP, Brazil
[e] Department of Materials Engineering, Universidade Federal de São Carlos, 13565-905 São Carlos, SP, Brazil
[f] Department of Mechanical Engineering, Pontifícia Universidade Católica do Paraná, 80215-901 Curitiba, PR, Brazil

ARTICLE INFO

Article history:
Received 20 July 2010
Received in revised form 28 March 2011
Accepted 29 March 2011
Available online 9 April 2011

Keywords:
Ceramics wear
Glass-ceramics
Corrosion wear
Nanoindentation
Tribology

ABSTRACT

Mechanical and tribological properties of a partially crystallized sintered glass-ceramic were compared to two commercial floor tiles: black granite and porcelainized stoneware. Mechanical properties, hardness and elastic modulus were evaluated by instrumented indentation. Friction coefficient and wear characterization were evaluated using a reciprocating ball-on-flat tribometer in two controlled environments: air with relative humidity of 53% and under running water at 23 °C. The sintered glass-ceramic and porcelainized stoneware presented similar mechanical and tribological properties. Regarding the mechanical and tribological properties, the results suggest that this glass-ceramic is suitable to be used as industrial tile.

1. Introduction

Glass-ceramics are produced by a controlled crystallization of glasses and have several industrial applications. Their properties can vary depending on the chemical composition of the precursor glass, the amount of crystalline phase, the amount of residual glass and the shape, the size and the distribution of crystals in the microstructure [1].

Glass-ceramic tiles for architectural use have increased commercial interest [2]. Glass-ceramic tiles have been developed and commercialized since the early 70s mainly based on wollastonite ($CaO{\cdot}SiO_2$) or making use of slag or other wastes as raw materials [3,4]. Since then, there have been significant efforts to find new compositions and fabrication processes for cheaper and/or visually attractive tiles, often tuned with the idea of ecologically sustainable industrial processes. Despite the industrial interest in applying glass-ceramics in tiles, tribological studies are scarce in the literature. One of the few articles published about this subject was written by Cranmer [5], where it was determined the friction coefficient values and the wear rate of the following commercial glass-ceramic compositions: Li_2O–MgO–ZnO–Al_2O_3–SiO_2 (stuffed β-quartz solid solution), Li_2O–Al_2O_3–SiO_2 (β-spodumene solid solution), Na_2O–Al_2O_3–SiO_2 (nepheline) and K_2O–MgF_2–MgO–SiO_2 (mica). The average friction coefficient values ranged from 0.07 to 0.49, measured on sample pairs of parallel rings. Cracking and ploughing occurred in different degrees in all samples. The materials produced debris with sizes smaller than or about the same size as the glass-ceramic microstructure crystallites. The wear rate was only measured for a stuffed β-quartz solid solution sample that resisted the experimental procedure. The reported wear rate was 43×10^{-14} m^3/N m.

Xiao et al. [6] studied the tribological properties of glass-ceramics prepared with industry slag having diopside ($CaO{\cdot}MgO{\cdot}2SiO_2$) and wollastonite ($CaO{\cdot}SiO_2$) as the crystalline phases. A Vickers hardness of 12 GPa was achieved for this glass-ceramic. Plate-to-plate wear tests were conducted in a dry friction device with 200 m sliding distance under different temperatures, contact pressures and sliding speeds. According to this study, the friction coefficient values increased with the increase of the contact pressure, tending asymptotically to a constant level. The authors suggest that the friction resistance is reduced due to increasing friction heat, which allows plastic deformation to occur at high speeds and high contact pressures. The specific wear rate at room temperature at 0.2 m/s increased with the contact pressure, ranging from 4×10^{-5} to 30×10^{-5} mm^3/N m at 0.1 MPa and 70×10^{-5} mm^3/N m at 0.4 MPa. For a constant contact pressure

* Corresponding author. Tel.: +55 41 3271 1346; fax: +55 41 3271 1349.
E-mail addresses: pa.soares@pucpr.br, pcsoaresjr@yahoo.com (P. Soares).

0043-1648/$ – see front matter
doi:10.1016/j.wear.2011.03.022

Table 1
Hardness (H_{IT}), elastic modulus (E_{IT}), specific wear rate (W), friction coefficient values (μ) and Archard coefficient (K) for glass-ceramic, porcelainized stoneware, and granite.

Properties		Materials			
		Glass-ceramic	Porcelainized stoneware	Granite (region 1)	Granite (region 2)
H_{IT} (GPa)		6.3 ± 0.2	6.4 ± 0.1	1.6 ± 0.4	8.7 ± 0.9
E_{IT} (GPa)		76.8 ± 2.9	75.7 ± 6.1	44.9 ± 8.9	90.7 ± 5.2
μ	*Dry*	0.55 ± 0.02	0.54 ± 0.03	0.28 ± 0.03	0.61 ± 0.01
W (mm^3/N m) × 10^{-6}		0.2 ± 0.05	0.9 ± 0.2	407.1 ± 91	0.7 ± 0.16
$K \times 10^{-3}$		0.0013 ± 0.0003	0.0056 ± 0.0011	0.6513 ± 0.1302	0.0065 ± 0.0013
μ	*Wet*	–	–	0.20	0.33
W (mm^3/N m) × 10^{-6}		9.0 ± 2.1	5.1 ± 1.1	632.4 ± 141.4	8.2 ± 1.8
$K \times 10^{-3}$		0.0565 ± 0.0113	0.0327 ± 0.0065	1.0118 ± 0.2023	0.0713 ± 0.0142

of 0.1 MPa, the specific wear rate decreased with temperature, from 1×10^{-3} mm^3/N m at 500 °C to 10^{-5} mm^3/N m at 800 °C. This was also observed for a higher a contact pressure of 0.4 MPa, the specific wear rate decreased from 2×10^{-3} mm^3/N m at 500 °C to 2.2×10^{-4} mm^3/N m at 800 °C.

In another work, Gant and Gee [7] studied the effect of tribochemical reaction on the sliding wear of ceramics. They concluded that the wear of the tested ceramic materials was significantly affected by the synergy of sliding wear and corrosion by the fluid.

The aim of this work was to evaluate the mechanical and tribological behavior of a new sintered glass-ceramic tile. This glass-ceramic has been developed using a readily available soda-lime-silica glass with an attractive mosaic-like macrostructure [8]. The properties of this material were compared to traditional materials such as black granite and porcelainized stoneware that are commonly used in the tile industry.

2. Experimental details

2.1. Glass-ceramic preparation

The glass-ceramic synthesis started with a crushed commercial soda-lime silica glass that was compacted into a refractory mold and heat-treated for simultaneous sintering and crystallization. Glass-ceramic monoliths with crystoballite (SiO_2) and devitrite ($Na_2O{\cdot}3CaO{\cdot}6SiO_2$) crystalline phases were obtained by the following process according to Zanotto et al. [8–10]: (a) milling the glass to an average particle size of approximately 5 mm; (b) compacting the particulate material in refractory molds; and (c) thermally treating the compact for viscous flow sintering with simultaneous crystallization at approximately 1000 °C. The heat treatments were designed and controlled in order to obtain partially crystallized materials.

The glass-ceramic samples were ground with SiC abrasive paper up to 1200 grit and polished with CeO_2 slurry and compared to polished commercial porcelainized stoneware and granite samples.

2.2. Mechanical properties

The hardness and elastic modulus of the materials under investigation were measured by instrumented indentation, where an indenter of known geometry is pressed into a material and the load penetration depth (h) is constantly recorded as a function of the applied load (P) for both the loading and the unloading cycle [11–14]. It was used a Nanoindenter XP (MTS Instruments) with a Berkovich tip. The applied load ranged from 3 to 400 mN corresponding to eight complete loading–unloading cycles. A set of 64 indentations (8 × 8) separated by a distance of 150 μm was done. The nanoindentation results are the average of these indentation sets. The hardness (H_{IT}) and elastic modulus (E_{IT}) were determined from the P–h curves applying the Oliver and Pharr method [15].

2.3. Tribological properties

The tribological properties were obtained from ball-on-flat reciprocating sliding method [16] in a CSM tribometer using a tungsten carbide (WC) ball with a diameter of 6.3 mm, with the following conditions: applied load of 5 N, stroke distance of 2 mm with a maximum sliding velocity of 2 cm/s and total sliding distance of 10 m. The WC ball was chosen as counterface because it provided a necessary wear severity that would facilitate comparing the materials wear resistance. The tests were conducted in two different controlled environmental conditions: 53% relative humidity at 23 °C and under running distilled water at 23 °C. These two conditions are named from now on as *Dry* and *Wet* conditions, respectively.

The friction coefficient value (μ) was continuously monitored during the experiments using the CMS-Instrument computer code. The specific wear rate (W) and Archard coefficient (K) were

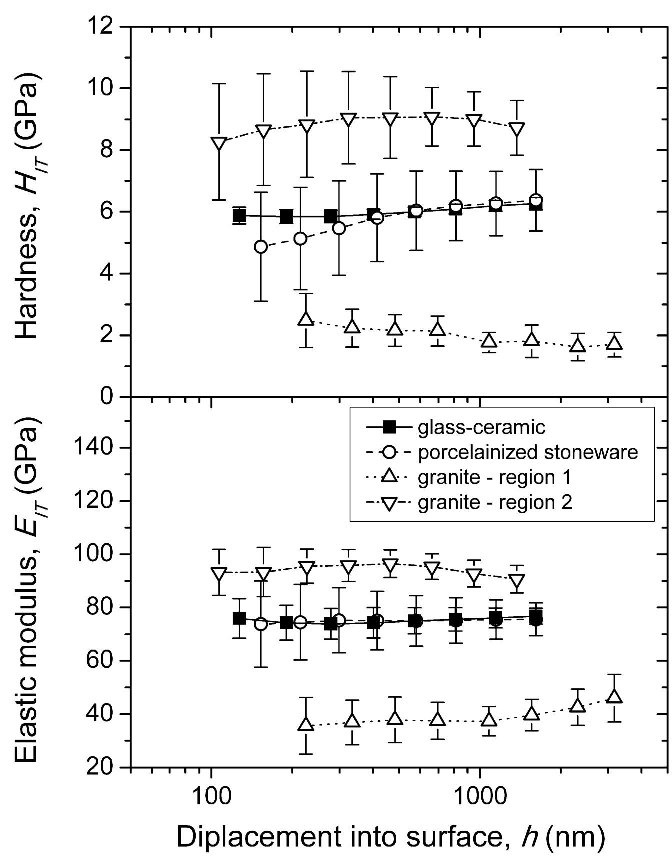

Fig. 1. Instrumented indentation hardness (H_{IT}) and elastic modulus (E_{IT}) as a function of penetration depth (h) of the glass-ceramic, porcelainized stoneware and granite.

obtained from the average of three measurements of cross section profile of the wear tracks, determined by the Nanoindenter XP in the profilometry mode with a Berkovich tip.

The specific wear rate (W) is defined by [17–19]:

$$W = \frac{V}{PL} \quad (1)$$

where W has the unit of volume loss per unit of force per unit of distance ($mm^3/N\,m$), P is the normal load, L is the sliding distance and V is the calculated volume assuming an elliptical wear profile and determined by the expression:

$$V = \frac{\pi}{2} whl \quad (2)$$

where w is the wear groove width (minor semi-axe), h is the wear groove depth (major semi-axe) and l is the wear track length.

The Archard coefficient (K) is widely used as an index of wear severity. K is the proportionality constant between real contact area, sliding distance and the wear volume [16,20,21]:

$$V = KA_rL = KL\frac{P}{H} \quad (3)$$

where V is the volume loss, A_r is the real contact area, L is the sliding distance, P is the applied load and H is the hardness of the softer surface.

3. Results and discussion

3.1. Mechanical properties

The hardness and the elastic modulus values as a function of tip penetration depth (h) for each material are shown in Fig. 1 and Table 1. The hardness values were 6.3 ± 0.2 GPa for the glass-ceramic, 6.4 ± 0.1 GPa for the porcelainized stoneware, 1.6 ± 0.4 GPa for the soft region of granite (region 1 composed by mica) and 8.7 ± 0.9 GPa for the hard region of granite (region 2 composed by quartz + feldspar). The elastic modulus values were 76.8 ± 2.9 GPa for the glass-ceramic, 75.7 ± 6.1 GPa for the porcelainized stoneware, 44.9 ± 8.9 GPa for the mica region and 90.7 ± 5.2 GPa for the hard region of granite.

It is observed that the average values of H_{IT} and E_{IT} are similar for the glass-ceramic and porcelainized stoneware but both are different from the two granite regions. The granite presents bimodal values depending on the indented phase (region 1 – mica, region 2 – quartz).

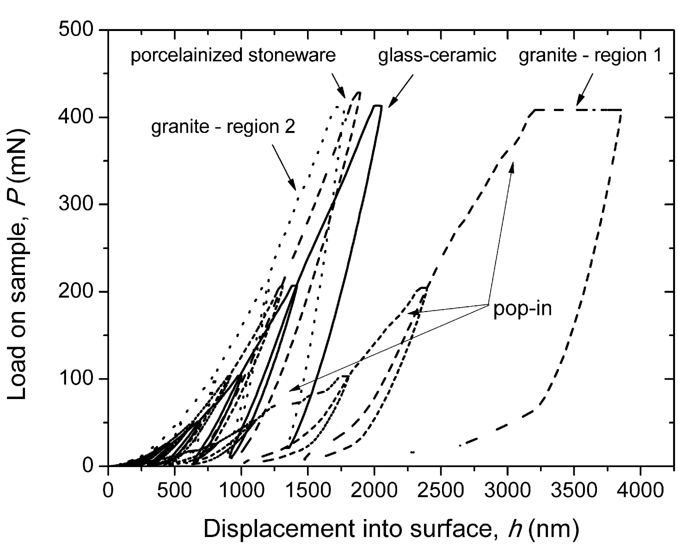

Fig. 2. Typical P vs h curves for the studied materials.

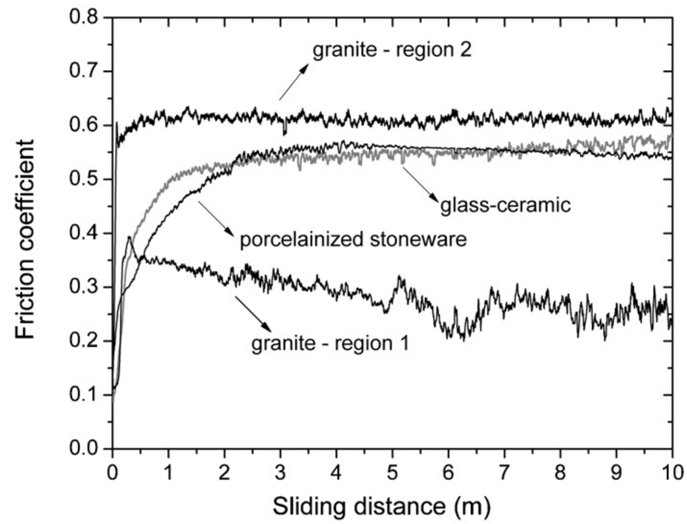

Fig. 3. Friction coefficient profiles of samples tested at 53% relative humidity and 23 °C with an applied load of 5 N. Total scratch length of 10 m.

For higher load penetration depth (h), the magnitude of the scattering in the H_{IT} and E_{IT} values was quantified by a statistical non-dimensional parameter or variation coefficient (VC) which can be determined by the relation $VC = (S/\bar{X}) \times 100\%$ [22]. Where S is the standard deviation and $\bar{X}$ is the average value of the hardness or elastic modulus for a given load penetration depth. The VC values found for the hardness and the elastic modulus were lower than 15% (except for the mica region in the granite), for an indentation depth superior to 1000 nm, which indicates that the values are statistically homogeneous [22].

Fig. 2 shows representative curves of load versus displacement into the surface of the three materials. A similar behavior is observed among glass-ceramic, porcelainized stoneware and hard region of granite. There is no occurrence of fracture events (pop-in) as observed in the soft region of granite (region 1). The mica has lamellar structure and the "pop-ins" in the indentation curves are related to the fracture of its layers during the loading as observed for other lamellar materials [23,24].

3.2. Tribological properties

The friction coefficient behavior as a function of the sliding distance is shown for both test conditions in Fig. 3 (*Dry*) and Fig. 4 (*Wet*) and Table 1. In the dry condition two different regimes are identified for all friction coefficient curves: a transient behavior, corresponding to the running-in period which corresponds to the accommodation between surface and ball followed by stationary regime in which materials removal takes place at a constant rate [16,25]. In the running-in regime the WC ball has low interaction with the sample, once the first contact with the ceramic surface occurs on the asperities and these asperities do not deform plastically. The stationary regime is characterized by a three body complex interaction involving the sample, the WC ball and the debris formed by particle fracture and delamination, as observed in the SEM images in Fig. 5.

The average friction coefficients values (μ) determined from the stationary regime for *Dry* conditions (Fig. 3) were 0.55 ± 0.02 for glass-ceramic, 0.54 ± 0.03 for porcelainized stoneware, 0.28 ± 0.03 and 0.61 ± 0.01 for mica and (quartz + feldspar) regions, respectively. The variation coefficient (VC) of the friction coefficient data indicates a good homogeneity of the data points with VC lower than 12%. A similar friction coefficient behavior is observed for the glass-ceramic and porcelainized stoneware while gran-

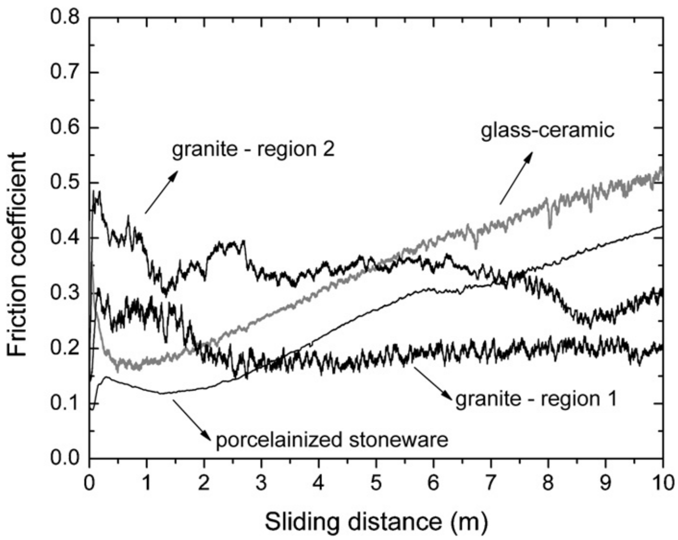

Fig. 4. Friction coefficient profiles of samples tested with running distilled water and 23 °C with an applied load of 5 N. Total scratch length of 10 m.

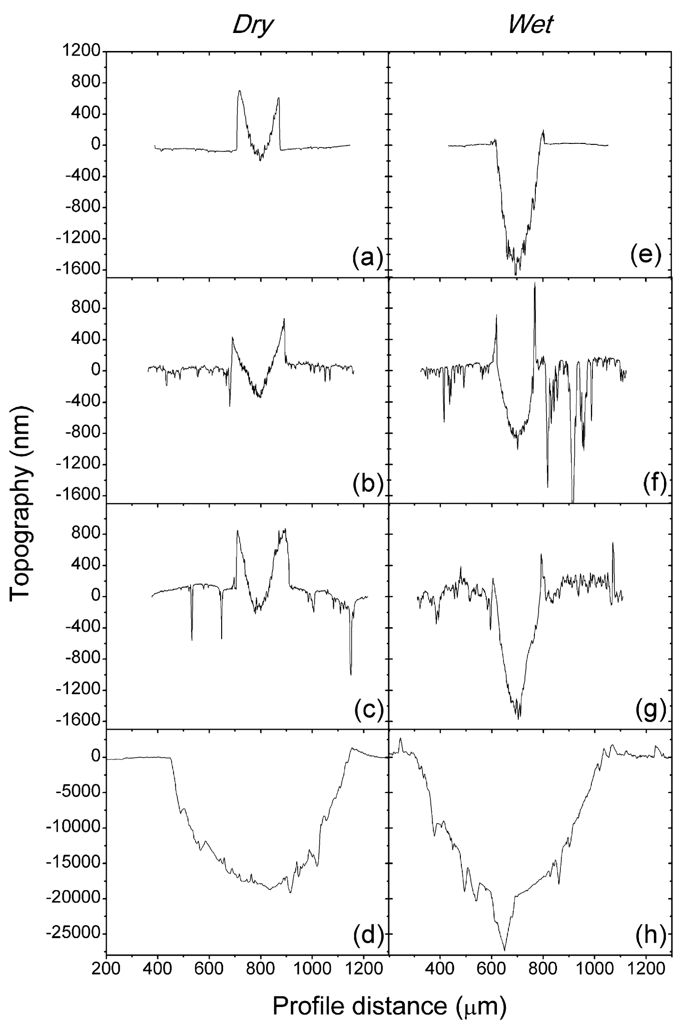

Fig. 5. Groove profiles obtained in the center of each wear track for both test conditions, *Dry* (53% relative humidity) and *Wet* (running water) at 23 °C. (a) Glass-ceramic – dry; (b) porcelainized stoneware – dry; (c) granite (region 2) – dry; (d) granite (region 1) – dry; (e) glass-ceramic – wet; (f) porcelainized stoneware – wet; (g) granite (region 2) – wet; (h) granite (region 1) – wet.

ite presents two different behaviors, depending on the tested region.

A completely different behavior for the friction coefficient is observed when the tribological tests are performed under running water as can be observed in Fig. 4. In the wet condition no stationary regime is reached for glass-ceramic and porcelainized stoneware up to the total sliding distance of 10 m, which means that there is a continuous dissolution of the surface in the aqueous solution due to tribochemical reactions between the glassy phase and water [26,27]. The interaction between the SiO_2 and water produces structural and chemical changes which implies in changes of the surface chemical composition. According to several authors [28], the reaction between glass and water happens in two stages. In the initial or primary stage, there is a substitution of the sodium ions by hydrogen ions from the water. In this stage there is no interaction between Si–O–Si bonds and hydrogen. In the second stage, there is a breakdown of the Si–O–Si bonds and a partial or total glass dissolution in the aqueous solution is observed. Fig. 4 shows that the glass-ceramic and porcelainized stoneware are more affected by this corrosion mechanism than the granite (region 2) due to the presence of a glassy phase. Moreover, the porcelainized stoneware and glass-ceramic present a short initial running-in (<1 m). For all materials, the friction coefficient value in the wet condition is lower than in the *dry* condition, which is attributed to a decrease in adhesive forces due to the lubricant effect of water. However, the wet friction coefficient value of the glass-ceramic, after a sliding distance of 10 m, tends towards the same value of the *dry* condition. The same behavior is observed for the porcelainized stoneware, but the friction coefficient value reached after 10 m is lower for the *wet* condition than for the *dry* condition.

Fig. 5 shows representative groove profiles obtained in the center of the wear tracks for both test conditions, *dry* (53% relative humidity) and *wet* (running water) at 23 °C.

For the *Dry*-condition test, the specific wear rate values (in 10^{-6} mm^3/N m units) were: 0.21 for glass-ceramic, 0.94 for porcelainized stoneware, 407.1 and 0.74 for mica (region 1) and feldspar + quartz (region 2), respectively. For *Wet* conditions, the values were 9.0 for glass-ceramic, 5.1 for porcelainized stoneware, 632.4 and 8.2 for mica and quartz + feldspar granite regions, respectively.

The Archard coefficient values (in multiples of 10^{-3}) for *Dry* and *Wet* conditions were respectively: 0.0013 and 0.0565 for glass-ceramic, 0.0056 and 0.0327 for porcelainized stoneware, 0.6513 and 1.0118 for mica region of the granite, 0.0065 and 0.0713 for feldspar + quartz region of the granite. These results are corroborated by the tribology results where it was observed that the wear of the porcelainized stoneware is higher than the glass-ceramic for *Dry* conditions. For *wet* conditions occurs the opposite, as the amount of glassy phase in glass-ceramic is higher than for porcelainized stoneware. This result suggests that a silicate dissolution process might be occurring.

The Archard coefficient (K) can also be assumed as the amount of asperity contacts resulting in wear. The K value is never supposed to exceed unity and, in reality, K has a value of 10^{-3} or less for all but the most severe forms of wear. The lower value of K indicates that wear is caused only by a very small amount of asperity contacts [21].

There is a distinct difference between the two sliding conditions, where the worn area tested for the *Dry* condition presents a relatively smoother surface as can be seen in Fig. 6. In the *Wet* condition wear was more severe resulting in deeper wear grooves as observed by the profiles of all materials and by the Archard coefficients. It is also possible to observe the presence of microfracture and surface delamination. Despite the lubricant effect of water, wear is related to crack growth induced by its tribochemical effects, and possibly due to the debris removal by running water.

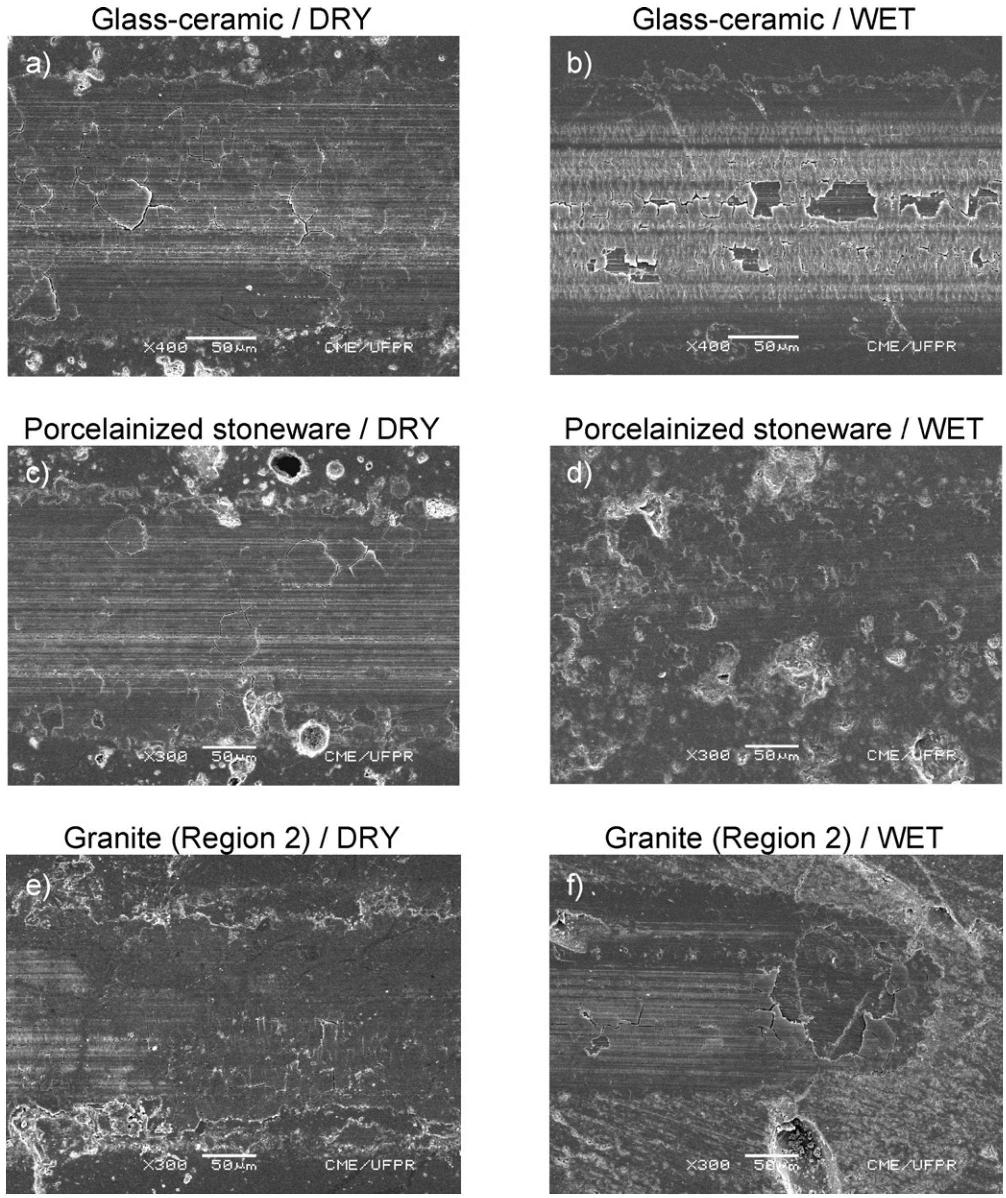

Fig. 6. SEM micrographs of the wear track for both test conditions, *Dry* (53% relative humidity) and *Wet* (running water) at 23 °C. (a) glass-ceramic – dry; (b) glass-ceramic – wet; (c) porcelainized stoneware – dry; (d) porcelainized stoneware – wet; (e) granite (region 2) – dry; (f) granite (region 2) – wet.

In summary, instrumented indentation, sliding friction and wear tests have been performed for three materials used as commercial tiles, including a sintered glass-ceramic, a commercial porcelainized stoneware and black granite. The results are summarized in Table 1.

4. Conclusions

The results showed that the sintered glass-ceramic and porcelainized stoneware present similar mechanical properties values (hardness and elastic modulus) and friction coefficients values under both conditions (*Dry* and *Wet*) and both presented better results than black granite.

Considering the specific wear rate, the glass-ceramic presented lower values than porcelainized stoneware for *Dry* conditions. This situation is the opposite for *Wet* conditions due to the fact that the glass-ceramic is more susceptible to damage by tribochemical effects.

Finally, the results show that the glass-ceramic produced from sintered commercial soda-lime glass could be used as industrial or architectural tile with the same application of the porcelainized stoneware.

Acknowledgements

The authors would like to thank CNPq, CAPES, and FAPESP (#2007/08179-9) for financial support, the Tribology Laboratory at Universidade Federal do Paraná for the use of its facilities. The authors are also grateful to Dr. C.E. Foerster for his helpful comments.

References

[1] W. Höland, G.H. Beall, Glass-Ceramic Technology, John Wiley & Sons – The Am. Ceram. Soc., Westerville, 2002.
[2] R.D. Rawlings, J.P. Wu, A.R. Boccaccini, Glass-ceramics: their production from wastes – a review, J. Mater. Sci. 41 (3) (2006) 733–761.

[3] S. Nakamura, Crystallized glass article having a surface pattern, US Patent 3955989, 1976.
[4] A. Karamanov, I. Gutzow, I. Penkov, Diopside marble-like glass-ceramics, Glass Sci. Technol. 67 (7) (1994) 202–208.
[5] D.C. Cranmer, Tribological properties of glass-ceramics, J. Am. Ceram. Soc. 67 (9) (1984) C180–C189.
[6] H. Xiao, Y. Cheng, Q. Yang, T. Senda, Mechanical and tribological properties of calcia–magnesia–alumina–silica-based glass-ceramics prepared by in situ crystallization, Mater. Sci. Eng. A 423 (1–2) (2006) 170–174.
[7] A.J. Gant, M.G. Gee, Sliding wear corrosion of ceramics, Wear 267 (2009) 599–607.
[8] E.D. Zanotto, E.B. Ferreira, C. Fredericci, M. O. Prado, Glass and glass-ceramic articles and process to prepare same, World Patent 2004/103921, 2004.
[9] E.D. Zanotto, M.O. Prado, Isothermal sintering with concurrent crystallization of monodisperse and polydispersed glass particles – Part 1, Phys. Chem. Glasses 42 (3) (2001) 191–198.
[10] M.O. Prado, C. Fredericci, E.D. Zanotto, Glass sintering with concurrent crystallization. Part II: non-isothermal sintering of jagged polydispersed particles, Phys. Chem. Glasses 43 (5) (2002) 215–223.
[11] J. Woirgard, C. Tromas, J.C. Girard, V. Audurier, Study of the mechanical properties of ceramic materials by the nanoindentation technique, J. Eur. Ceram. Soc. 18 (15) (1998) 2297–2305.
[12] C. Ullner, J. Beckmann, R. Morrell, Instrumented indentation test for advanced technical ceramics, J. Eur. Ceram. Soc. 22 (8) (2002) 1183–1189.
[13] C.M. Lepienski, C.E. Foerster, Nanomechanical properties by nanoindentation, in: H.S. Nalwa (Ed.), Encyclopedia of Nanoscience and Nanotechnology, American Scientific Publishers, Stevenson Ranch, 2004, pp. 1–20.
[14] M.R. Van Landingham, Review of instrumented indentation, J. Res. Natl. Inst. Stand. Technol. 108 (4) (2003) 249–265.
[15] W.C. Oliver, G.M. Pharr, Measurement of hardness and elastic modulus by instrumented indentation: advances in understanding and refinements to methodology, J. Mater. Res. 19 (1) (2004) 3–20.
[16] B. Bhushan, B.K. Gupta, Handbook of Tribology: Materials, Coating and Surface Treatments, McGraw-Hill, New York, 1991.
[17] P.J. Blau, R.L. Martin, E.S. Zanoria, Effects of surface grinding conditions on the reciprocating friction and wear behavior of silicon nitride, Wear 203–204 (1997) 648–657.
[18] D. Jianxin, D. Zeliang, Z. Jun, L. Jianfeng, C. Tongkun, Unlubricated friction and wear behaviors of various alumina-based ceramic composites against cemented carbide, Ceram. Int. 32 (5) (2006) 499–507.
[19] C. Liu, J. Zhang, J. Sun, X. Zhang, Tribological properties of pressureless sintered alumina matrix ceramic materials improved by diopside, J. Eur. Ceram. Soc. 28 (1) (2008) 199–204.
[20] J.F. Archard, Single contacts multiple encounters, J. Appl. Phys. 32 (1961) 1420–1425.
[21] G.W. Stachowiak, A.W. Batchelor, Engineering Tribology, Second ed., Elsevier-Butterworth-Heineman, 2000, pp. 468–478.
[22] M.S. Bobji, K. Shivakumar, H. Alehossein, V. Venkateshwarlu, S.K. Biswas, Influence of surface roughness on the scatter in hardness measurements – numerical study, Int. J. Rock Mech. Min. Sci. 36 (3) (1999) 399–404.
[23] C.M. Lepienski, M.S. Meruvia, W. Veiga, F. Wypych, Mechanical properties of niobium disulfide and its hydrated sodium cation intercalation compound, J. Mater. Res. 15 (10) (2000) 2069–2072.
[24] A. Mikowski, P. Soares, F. Wypych, J.E.F.C. Gardolinski, C.M. Lepienski, Mechanical properties of kaolinite macro-crystals', Philos. Mag. 87 (29) (2007) 4445–4459.
[25] C. Djelal, Designing perfecting a tribometer for the study of friction of a concentrated clay–water mixture against a metallic surface, Mater. Struct. 34 (1) (2001) 51–58.
[26] T.A. Michalske, B.C. Bunker, The fracturing of glass, Sci. Am. 257 (1987) 122–128.
[27] M. Tomozawa, Fracture of glasses, Annu. Rev. Mater. Sci. 26 (1996) 43–74.
[28] D.E. Clark, C.G. Pantano Jr., L.L. Hench, Corrosion of Glass, Ed. Books for Industry and The Glass Industry, 1979, 75 p.